Heat transport by long mean free path vibrations in amorphous silicon nitride near room temperature

Rubina Sultan, A. D. Avery, J. M. Underwood, S. J. Mason, D. Bassett, and B. L. Zink

Phys. Rev. B **87**, 214305 — Published 24 June 2013

DOI: 10.1103/PhysRevB.87.214305

Heat transport by long mean free path vibrations in amorphous silicon nitride near room temperature

Rubina Sultan, A. D. Avery, J. M. Underwood, S. J. Mason, D. Bassett, and B. L. Zink*
Department of Physics and Astronomy, University of Denver
(Dated: June 6, 2013)

We present measurements of thermal transport in 500 nm thick, 35 μm wide and 806 μm long micromachined suspended silicon nitride (Si-N) bridges over the temperature range of 77–325 K. The measured thermal conductivity of Si-N (for material grown by LPCVD in two different furnaces) deviates somewhat from previously reported measurements and also shows surprising dependence on surface variation at these relatively high temperatures. Addition of discontinuous gold films causes the thermal conductance of Si-N bridges to drop through the entire measured temperature range, before rising again when thicker, continuous films are added. Similar effects occur when continuous, but very low thermal conductivity alumina films are deposited. The reduction in thermal conductance upon modification of the Si-N surface is strong evidence that vibrational excitations with long mean free paths carry significant heat even at these high temperatures. By measuring a series of film thicknesses the surface-scattering effects can be mitigated, and the resulting experimental values of the thermal conductivity of alumina and Au thin films compare very well to known values or to predictions of the Wiedemann-Franz law. We also present a modified model for the phonon mean free path in thin film geometries, and use it along with AFM scans to show that a very small population of phonons with mean free path on the order of 1 μm and wavelength much longer than expected thermal wavelengths carry up to 50% of the heat in Si-N at room temperature.

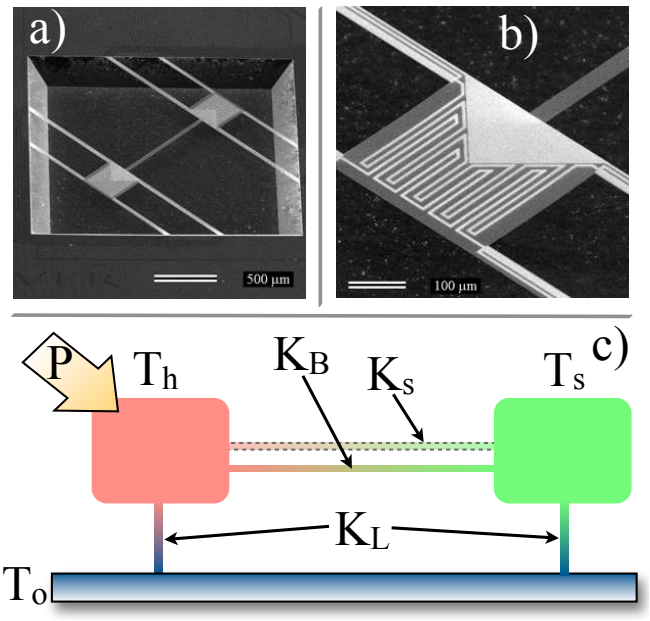

FIG. 1. **a)** A tilted SEM micrograph of the suspended Si-N thermal platforms. Here two 250 x 250 μm^2 Si-N islands are connected to a Si frame by eight Si-N legs and also connected together by a 806 μm long, 35 μm wide, 500 nm thick Si-N suspended bridge. Metal film thermometers and heaters, each with four leads directly to the thermometer element, are patterned on each island. A similar thermometer is also patterned on the chip to monitor the reference temperature, T_o. **b)** A closer view of one of the islands, depicting the patterned metal (Mo) heater and thermometer meanders. Two triangular metal (Mo) leads on each island allow for thermopower measurements (not described here), **c)** Thermal model representing the thermal isolation platform, as described in the main text.

I. INTRODUCTION

Recent experimental and theoretical work is challenging long-held views of what type of phonons carry heat in materials at room temperature. The usual picture of phonon thermal transport is that the dominant carriers of heat at a given temperature T have wavelength $\lambda_{\rm dom} = hv/4.25k_{\rm B}T$ where h and $k_{\rm B}$ are the Planck and Boltzmann constants and v is the speed of sound in the material,[1] and that at high temperatures phonon mean free path, ℓ, is on the order of several to tens of nanometers. However, new experimental techniques that probe thermal transport as a function of ℓ have shown unexpectedly large contributions to the high temperature thermal conductivity, k, of crystals from low frequency excitations with ℓ as long as microns.[2–6] Even more surprising, recent reports suggest that for at least one highly disordered material, a significant fraction of heat is carried by phonons with long ℓ at room temperature. Liu, et al. presented experimental evidence that phonons with $162 < \ell < 612$ nm were responsible for as much as 40% of the thermal transport in an amorphous silicon (a-Si) sample at 300 K.[7] In theoretical work based on non-equilibrium molecular dynamics simulations, He, Donadio, and Galli concluded that propagating vibrational modes (similar to the typical understanding of a phonon) with ℓ on the order of one micron, despite comprising only $\simeq$ 3% of the total number of active modes in a-Si at room temperature, are responsible for roughly half the heat conduction in a-Si.[8]

Thermal conductivity is often viewed as an intrinsic material-dependent property, though significant deviation in k from bulk behavior is common in low dimensional or nanoscale materials.[9–11] Surface scattering is known to play a role in thermal transport at low temperatures when ℓ grows to become comparable to the sample dimensions and long λ phonons unquestionably dominate. In this regime when phonons scatter specularly off the sample surface, ℓ can grow larger than the sample size. However, when this scattering is diffuse ℓ is limited and thermal transport in the material is similarly limited. In earlier work, the decoration of the surface of a square-shaped amorphous Si-N membrane with Ag particles caused up to a factor of 5 reduction of thermal conductance below 4 K.[12] Reduction in thermal conductance at low temperatures has also been observed in similar experiments on crystalline insulators when an initially clean surface was altered via thin film deposition[1,13]. If long ℓ phonons carry a significant amount of heat in Si-N at higher T, micromachined structures should show evidence of surface scattering effects even at room temperature. Demonstrating these effects is the main focus of this paper.

Heat conduction by long wavelength modes in disordered materials is not only of fundamental interest, but also

impacts applications from from quantum computation[14–16] to thermoelectric materials[9,10,17] to detectors for cutting-edge cosmology[18–20] or nuclear security[21,22]. For example, some of the most advanced detectors of radiation are thermal detectors that use highly sensitive micromachined thermometers to register the temperature rise caused by absorption of incident light or particles.[20,23] To achieve this sensitivity, the thermometer is commonly thermally isolated using free-standing amorphous silicon nitride membranes formed from material with low residual stress that is typically grown using Low Pressure Chemical Vapor Deposition (LPCVD)[24,25]. Furthermore, suspended Si-N membrane structures form the basis of sensitive micro- and nanocalorimeters, which are used for accurate thermodynamic measurements of thin solid films and liquid droplets.[26–29] Thus, understanding and predicting heat flow behavior in Si-N is critical to the design and development of a wide range of state-of-the-art sensing platforms.

In this paper, we first present measured thermal conductance, K, and thermal conductivity, k, of a large number of 500 nm thick suspended Si-N bridges in the temperature range of 77-325 K. We then demonstrate the effect of surface variation on the heat conduction in these bridges as a function of temperature. We use deposition of a series of Au films starting at the discontinuous limit and deposition of very low thermal conductivity alumina films as a means to explore the effects of surface scattering on thermal transport. We see very clear evidence that modification of the Si-N surface changes the transport of heat in the structure, indicating the importance of long ℓ modes for heat conduction in the material. We use AFM images and a modified model of surface scattering in a thin film to determine ℓ, the fraction of diffuse surface scattering, and an estimate of λ for the surface-sensitive phonons in Si-N. We also present k and Lorenz number, L, for several thin gold films, and k for a 200 nm thick alumina film.

II. EXPERIMENTAL TECHNIQUE

We measure thermal transport using the thermal isolation platform shown in Fig. 1. Here two Si-N islands are suspended over a Si-etch pit via eight Si-N legs. The thermal link between these two islands is an 806 μm long, 35 μm wide bridge fabricated from a nominally 500 nm thick layer of Si-N. All thermal platforms used in this set of experiments were fabricated from Si-N grown by LPCVD directly on Si wafers without an additional SiO_2 spacer layer. We used anisotropic Si etching with KOH to release the Si-N thermal isolation structure for these groups of platforms. We have previously reported more details of our techniques and k of Si-N measured using three platforms,[30] as well as measurements of k and thermopower of several metal films[30–32]. Because measurements of K of the Si-N bridge are made without the need to subtract large contributions from thermal conductance of metallic leads or radiation, our measurements are much more sensitive than others made using micromachined structures with different geometries[33]. This is a major advantage of the design of our platforms.

Measurements of the K of this bridge are made by measuring the temperatures of the heated island,T_h, the cooler island, T_s, and reference T_o as a function of power, $P = I_h V_h$, applied by flowing current I_h through the heater on one island. The resulting voltage on the heater V_h provides measurement of P. We determine temperature from measured and calibrated resistance of metal meanders function of T. Each heater and thermometer has four points of contact to allow the most accurate measurement of resistance. According to the thermal model shown in Fig. 1c, measurements of T_h and T_s as a function of applied heating power, P, allow calculation of K through the bridge, $K_{\rm B}$, and legs, $K_{\rm L}$, from linear fits to

$$T_h = T_o + \left[\frac{(K_L + K_B)}{(2K_B + K_L)K_L}\right] P, \tag{1}$$

$$T_s = T_o + \left[\frac{K_B}{(2K_B + K_L)K_L}\right] P. \tag{2}$$

$K_{\rm B}$ is converted to k for Si-N using the bridge geometry, $k_{\rm Si-N} = K_{\rm B} l/wt$, where l, w, and t are the length, width and thickness of the bridge, respectively. For all bridges discussed in this paper, $l = 806$ μm, $w = 35$ μm, and $t = 500$ nm. We maintain vacuum of $\approx 7 \times 10^{-7}$ Torr throughout the measurement. To measure k of a deposited film we first determine the bridge thermal conductance $K_{\rm B,Si-N}$, for the bare Si-N. Next, we deposit a film and again determine $K_{\rm B}$. By then subtracting $K_{B,\rm Si-N}$ as a background , we obtain $K_{B,\rm film}$, which along with knowledge of film geometry, allows a measurement of $k_{\rm film}$.

Au films were deposited either via thermal evaporation at base pressure $\sim 10^{-6}$ Torr, or via e-beam evaporation in a UHV chamber at pressures of $\sim 10^{-8}$ Torr or lower. Low-conductivity disordered alumina films were deposited via UHV e-beam evaporation from Al_2O_3 source material. Films were deposited both on the thermal platforms and on standard Si-N coated Si substrates, which were used for profilometry, AFM, and four-wire electrical resistivity measurements. Atomic Force Microscopy was performed with an Asylum MFP3D instrument in tapping mode and

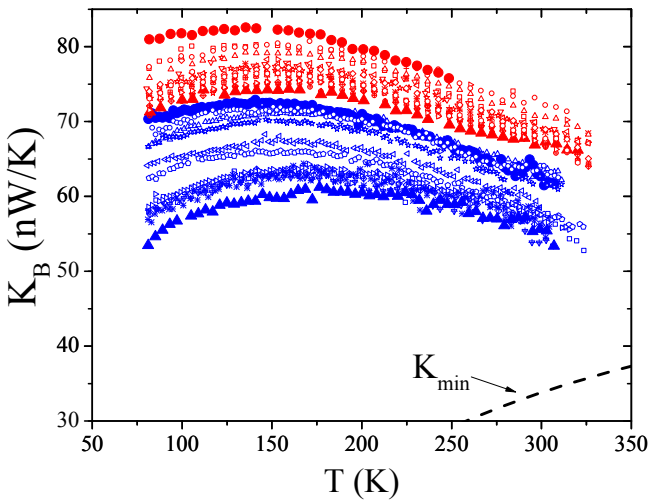

FIG. 2. Measured K_B as a function of T for a group of 500 nm thick Si-N bridges fabricated on two substrate wafers represented by red and blue symbols. The larger filled circles (triangles) indicate the largest (smallest) values measured for each wafer. The dashed line indicates K_{min} as discussed below.

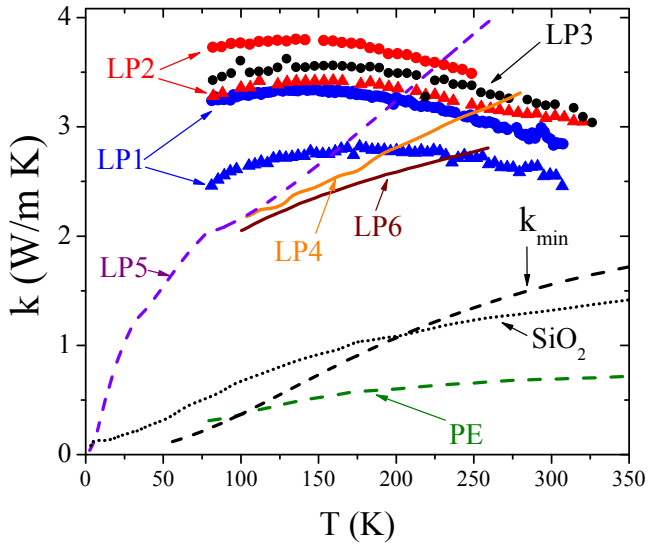

FIG. 3. k of Si-N vs. T determined from our thermal platform measurements compared to previously reported values of similar material. LP1 (blue symbols) and LP2 (red symbols) indicate Si-N grown at NIST Boulder, with circles (triangles) representing the maximum (minimum) measured values from the data shown in Fig. 2. LP3 (solid black circles) represents values from a Si-N thermal platform fabricated from material grown at UC Berkeley. All of these samples have very similar temperature dependence. Previously reported values for LPCVD Si-N include LP4[35], LP5[36], and LP6[37]. One sample made by PECVD (PE)[38] and vitreous silica (SiO_2)[39] are shown for comparison. k_{min} is the calculated minimum thermal conductivity for Si-N, and far below all values for material grown via LPCVD

analyzed with the free Gwyddion software package.[34]

III. RESULTS

Figure 2 shows the measured thermal conductance, K_B for more than twenty suspended silicon nitride bridges. These were fabricated on two different wafers, meaning that the suspended structure is formed from silicon nitride grown by the same technique at two different times. The estimated error on each of these thermal conductance measurements is ~ 0.4 nW/K at the low temperature end and ~ 1 nW/K at room temperature.

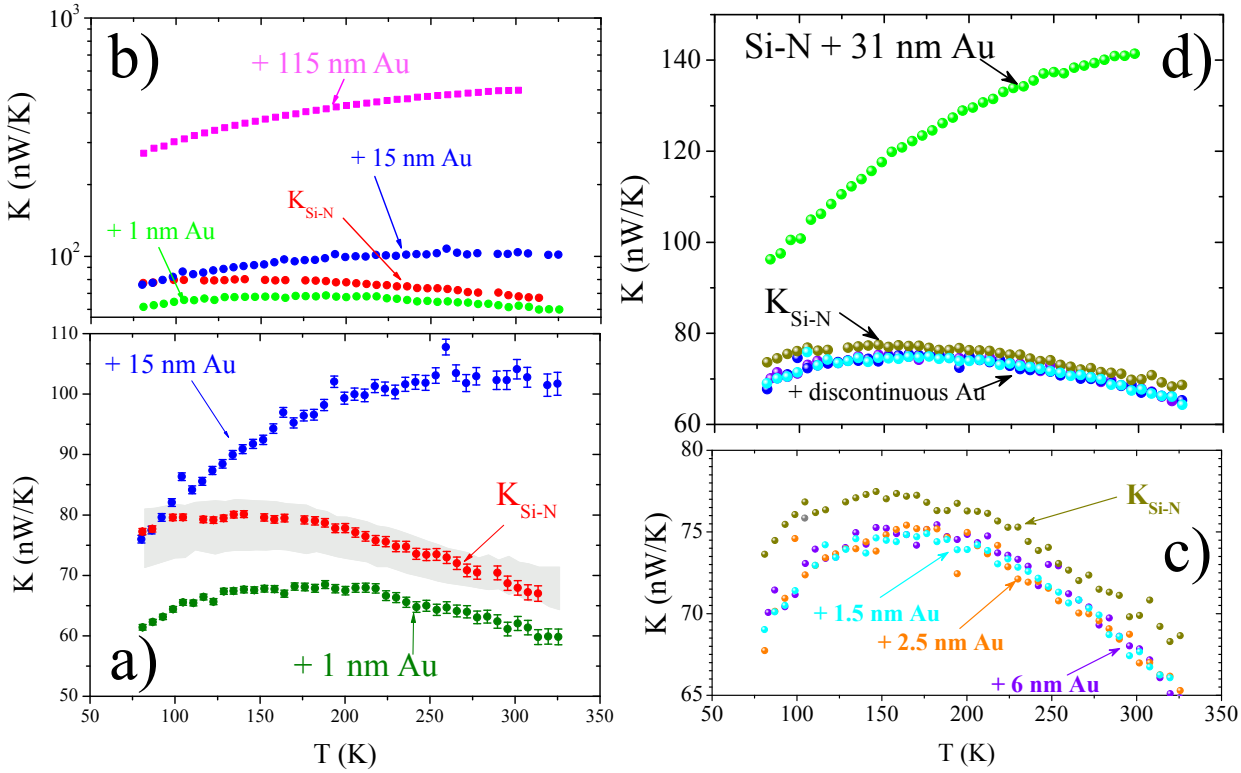

FIG. 4. (a) A plot of K vs. T compares initial values (red circles) to those measured after deposition of a discontinuous Au layer with average thickness of 1 nm (green circles), and after deposition of a second layer 15 nm thick. The shaded region indicates the spread of all values of K measured for bridges on the same wafer. **b)** K (on a log axis) vs. T for the same bridge after depositing a third, 100 nm Au film (pink squares) compared to the first three measurements. The thick film, as expected contributes a very large thermal conductance. **c)** K vs. T for an additional bridge shows initial values, and clear saturation of the drop in K upon adding subsequent thin Au films. **d)** Addition of a continuous 25 nm thick film again increases total K.

There are three striking features about these sets of data. First, as we discuss in more detail below, the shape of the curve as a function of temperature differs somewhat from the normal dependence expected in amorphous insulators. Second, there is a spread in K much larger than the experimental error in the values for bridges fabricated on the same wafer. The range in values is roughly 10 nW/K near room temperature and grows slightly at low temperatures. This is somewhat surprising since the photolithography used to define these features generates very uniformly sized structures. Third, the two groups of bridges fabricated from nominally identical materials and methods have rather different values. We note here that both the spread in the values and the shift from wafer to wafer are on the order of tens of nW/K. Previous methods of measurement of K and k for silicon nitride membranes report uncertainties on the order of μW/K[33,36], and are therefore not sensitive to the very small changes that we have identified.

Despite their small size, these changes from bridge-to-bridge and wafer-to-wafer were unexpected. One possible cause for the variation in apparent k could be a thickness variation of the Si-N layer across the wafer. However, the measured Si-N thicknesses typically deviate less across the wafer than the spread in thermal conductance. We have also ruled out measurement inaccuracy or variation by repeated measurements of a single bridge on several occasions. When no physical process changes a Si-N structure, repeated measurements agree within the estimated error bars shown in Fig. 2, even after removing the sample from the cryostat and remeasuring many weeks later (see Supplemental Material).

Figure 3 compares the thermal conductivity of Si-N determined from five measurements of our suspended Si-N bridges [LP1 (hollow circles), LP2 (hollow triangles), and LP3 (solid circles)] with previously reported measurements for amorphous Si-N films grown using LPCVD[35–37] and plasma-enhanced CVD (PECVD)[38], as well as to vitreous silica (SiO_2)[39]. As we initially reported for a small set of bridges in a previous publication,[30] though the magnitude of k is in the same range as previous measurements, there is an obvious departure of the temperature dependence both from that seen in previously measured LPCVD Si-N films and from the behavior typically seen in insulating thin films[40]. In materials grown using LPCVD in two different furnaces, one at NIST Boulder and the second at UC Berkeley, k is relatively flat throughout the $77-350$ K temperature range, and without the gradual increase at higher

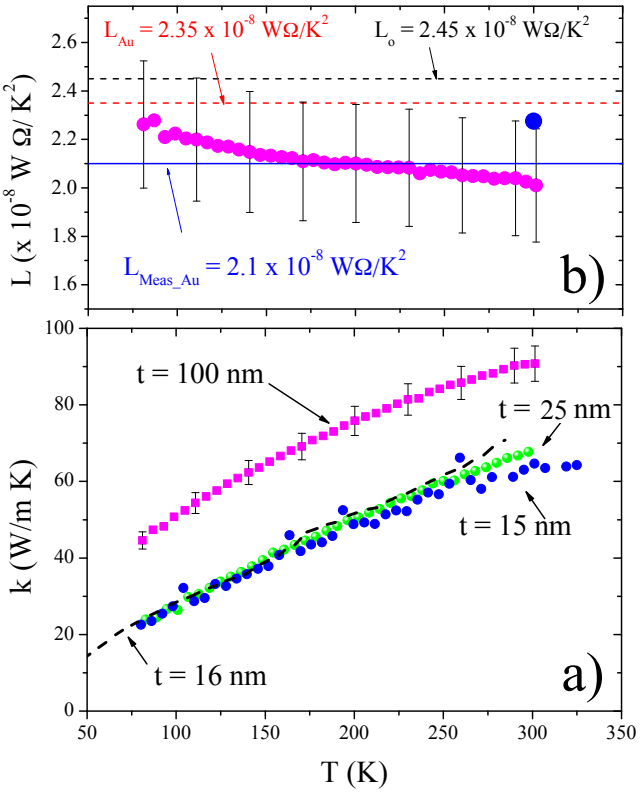

FIG. 5. **a)** k vs. T for the three continuous Au films shown in Fig. 2. Also shown (dashed line) is earlier work on k measured on a 16 nm film using a different micromachined device.[47] **(b)** Comparison of measured Lorenz number for the 100 nm (pink circles) and 15 nm (blue circle at 300 K) Au films with the Sommerfeld value ($L_o = 2.45 \times 10^{-8}$ WΩ/K^2) and the literature value for Au ($L_{Au} = 2.35 \times 10^{-8}$ WΩ/K^2). The average of the measured values is $L_{\mathrm{meas-Au}} = 2.1 \times 10^{-8}$ WΩ/K^2.

temperatures often seen in disordered insulators. Note however, that the normal expectation is that the average phonon mean free path will drop near room temperature toward some eventual saturation at a length comparable to the interatomic distance. The drop in k in this temperature range does not change this physical picture, it only suggests a more rapid drop in ℓ. The minimum thermal conductivity[41,42] is calculated here for Si-N using the atomic number density determined from the mass density $\rho = 2.9$ g/cm^3 and average molar mass of 21 g/mol, and transverse and longitudinal sound speeds in similar Si-N[12,43]. As discussed further in Sec. III A, the very poor match of all measured k for Si-N to k_{min} is unusual for an amorphous insulator.

We offer two further comments regarding the slight peak seen in k for the suspended Si-N bridges. The first is that the peak is small enough that it could be viewed merely as a somewhat broader than typical "plateau," another canonical signature of thermal conductivity in disordered insulators (consider that k data for insulators is most often compared on a log-log plot over broad ranges, which would make these slight peaks much less pronounced). However, a second possibility is that the nominally amorphous Si-N material is not utterly without order, but has some micro- or nano-crystalline nature. As we previously reported, there is some preliminary evidence from X-ray diffraction suggesting the presence of such crystallites.[30] In this light one can view the slight peak as a blend of the normal amorphous plateau with the precursor of the peak seen in k for crystalline materials. This sort of behavior indeed has been previously observed in fine-grained polycrystalline materials.[44,45] According to some reports, it is possible for such variations in the micro- and nano-crystalline nature of a material to lead to random variations in the apparent thermal conductivity.[46] One possible explanation for the variations in K and k that we see in these bridges could therefore be due to these structural deviations. However as the results we present below show, a strong sensitivity to the nature of the surface of the bridges is another likely factor.

Fig. 4 shows the effect of deposition of discontinuous Au films on the Si-N surface. Fig. 4a compares the initially measured bridge thermal conductance, labeled $K_{\mathrm{Si-N}}$ to values measured after UHV e-beam deposition of a discontinuous Au film with average thickness 1 nm (labeled "+ 1 nm Au") and a continuous film 15 nm thick. The shaded region around $K_{\mathrm{Si-N}}$ indicates the entire range of measured K for bridges fabricated from the same wafer shown in Fig. 2. The discontinuity of the Au layer was confirmed both by AFM analysis of the Au surface on the substrate, shown in Figure 9(b), and by electrical resistance. The addition of the Au asperities caused an easily measurable

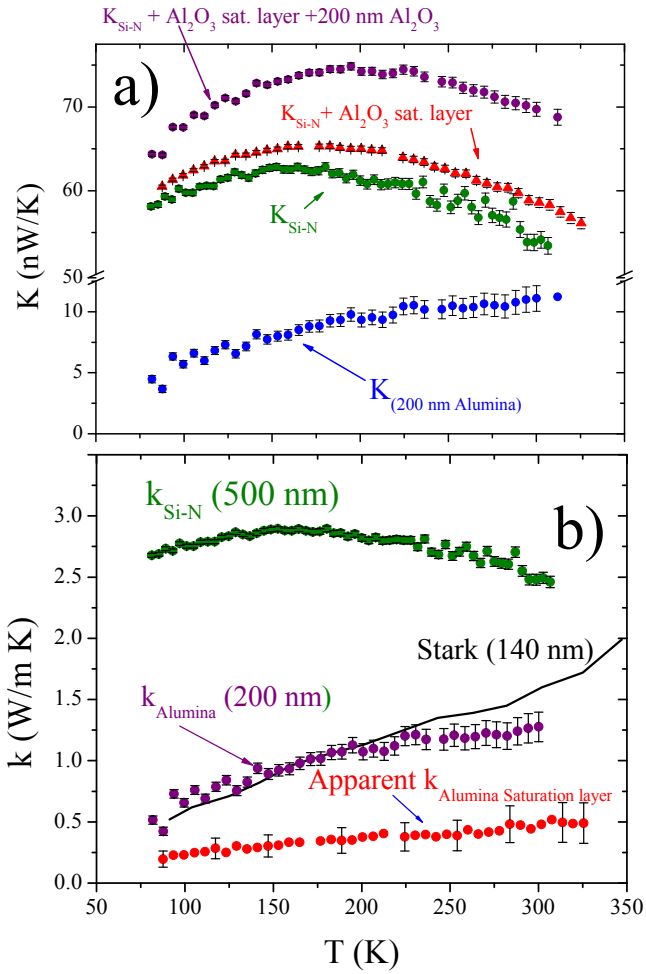

FIG. 6. a) Total measured thermal conductance of a 200 nm of alumina film compared with the Si-N background, thermal conductance of Si-N with alumina saturation layer, and the thermal conductance through 200 nm alumina film, (b) Measured thermal conductivity of a 200 nm thick alumina compared with $k_{\mathrm{Si-N}}$, the apparent thermal conductivity of the saturation layer and the literature value of k_{Alumina}.[48]

drop in K that is well outside both error bars and the range K of all bridges measured on this wafer. The additional 15 nm of gold is continuous and increases K as expected. Fig. 2b shows K vs. T for the same bridge after thermal evaporation of a final 100 nm layer of Au. Fig. 2c-d are results of a similar experiment on a different bridge (fabricated from Si-N grown at UC Berkeley). Fig. 2c shows K for the bare Si-N, and after three consecutive discontinuous gold depositions. After an initial drop due to the first 1.5 nm average thickness film, K is unchanged after addition of 1 nm (for total thickness 2.5 nm) and 3.5 nm (total thickness 6 nm) of Au. This shows a clear saturation of the surface scattering effects. Again, deposition of an additional 25 nm (for total thickness 31 nm) creates a continuous film with a large contribution to the total K.

Fig. 5a shows k determined from the continuous films described in Fig. 4. Here, each film uses the previous total K as the background for subtraction. This gives k for each of the layers of the film separately. As expected, k is highest for the thickest film. The 25 and 15 nm thick Au films have very nearly equal k, though the thinner film was prepared in a UHV chamber and likely is somewhat cleaner, explaining the apparent lack of dependence on thickness for these two films. A 16 nm thick film measured with a different style of calorimeter is also shown.[47] Fig. 5b shows Lorenz number, $L = k/\sigma T$ as a function of T for the 100 nm film, and at room temperature for the 15 nm film. For these films σ was determined from measurements on Si-N coated Si substrates (the matching substrate for the 25 nm film was damaged during handling). The error shown takes into account the uncertainty in sample geometry and thickness of the films. Both films agree, and are somewhat lower than both the Sommerfeld value, L_o, and the bulk value reported for Au.

We also investigated these surface effects by deposition of continuous, but very low thermal conductivity, electrically

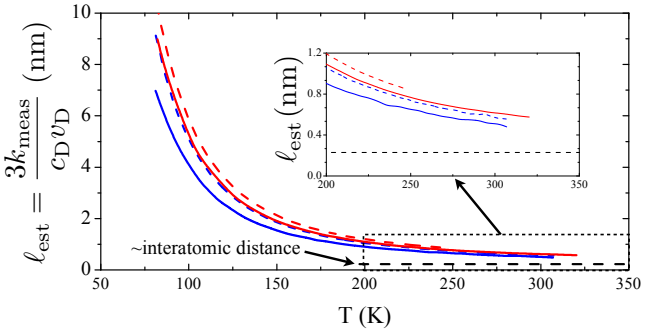

FIG. 7. Estimation of ℓ calculated from $3k_{\rm meas}/c_{\rm D}v_{\rm D}$. Colors match data shown in Figs. 2 and 3, with dashed (solid) lines indicating maximum (minimum) values of $k_{\rm Si-N}$ for each wafer. This shows the rough features expected, but (as shown in inset) fails to reach the average interatomic distance.

insulating films. This is a direct test of the procedure needed to accurately measure the thermal conductivity of such low k thin films. We deposited a 200 nm alumina (amorphous Al_2O_3) "saturation" layer on a pre-measured Si-N bridge and measured K. Measured K before and after deposition of the saturation layer is shown in Fig. 6(a). K is indeed only slightly higher after this first 200 nm alumina layer is added, indicating that $K_{\rm B}$ again dropped by approximately 7 nW/K due to the presence of the film on the top surface. To find the true K of thin film alumina we then deposited a second 200 nm thick film, and used the previous measurement as the background. The second 200 nm layer caused a much larger additional K. Subtracting the saturated background conductance and scaling for geometry gives k for thin-film alumina.

Figure 6(b) compares the resulting k of this second 200 nm alumina film to available literature values as well as the apparent (and certainly incorrect) k of the alumina saturation layer determined by subtraction of the inital $K_{\rm Si-N}$ from the values for the first 200 nm film. The apparent values for this first layer are clearly artificially low due to the surface-scattering induced changes in the Si-N background. However the values for the second layer agree very well below 200 K with previously reported data on an alumina film.[48]. The film in this previous study was prepared by anodic oxidation and was measured using steady state heat flow. The additional k at high temperatures could very well be due to radiation effects which are very difficult to eliminate at high temperatures when larger heated structures are used. We believe this series of experiments demonstrates the most effective way to measure k in low thermal conductivity materials with micromachined thermal platforms.

A. Discussion: Estimation of Contribution from Long Mean Free Path Modes

The experiments presented above confirm that thermal transport in suspended Si-N bridges is sensitive to the condition of the surface of the structures. This argues that a fraction of the excitations that carry heat in the disordered Si-N, even at room temperature, interact directly with the surfaces of the structure, and therefore must have long ℓ and correspondingly long λ. As mentioned earlier, recent experimental and theoretical work reports similar results for amorphous silicon,[7,8] where vibrational modes with ℓ in the range which would allow interaction with the surfaces of our bridges (on the order of several hundred nm) carries as much as $40-50\%$ of the heat current.

Figure 7 shows estimated values for the phonon mean free path, $\ell_{\rm set}$, calculated in the manner common in the disordered insulator literature and previous work on Si-N membranes[33,40]:

$$\ell_{\rm est} = \frac{3k_{\rm meas}}{c_{\rm D}v_{\rm D}}. \tag{3}$$

Here $k_{\rm meas}$ is the measured k of the Si-N bridges, $v_{\rm D}$ is the average sound velocity determined from measurements on similar Si-N films, and $c_{\rm D}$ is the Debye heat capacity using $\theta_{\rm D} = 985$ K based on the same sound velocity[33]. This estimation assumes that the heat-carrying modes are the transverse and longitudinal acoustic modes described reasonably well for low crystal momentum q by the Debye model. The results are similar to that seen in other glassy insulators, with values on the range of nanometers and an approach to saturation, seen in a closer view in the inset to Fig. 7. However, in most materials $\ell_{\rm est}$ saturates nearer to the interatomic spacing near room temperature. The $\sim 2-3\times$ higher saturation in Si-N is again evidence of unusual phonon transport due to far larger than expected contributions from long-wavelength modes. It is also clear that $\ell_{\rm est}$ does not give a complete view of the mean free paths of all the important phonons, since mean free paths of the order of nm can not explain the sensitivity to surface

modification.

As shown in Fig. 3, measured k in the Si-N bridges exceeds the calculated $k_{\rm min}$ by as much as a factor of 2.2 at room temperature. This large excess heat conductivity is seen in no other disordered materials, and only roughly matched by some bulk crystals.[41,49] Assuming that this contribution is due to the long λ surface-sensitive modes, using our results we can estimate ℓ, λ and the number of these modes by determining the fraction of diffuse surface scattering at each surface, f. This approach requires a more careful determination of ℓ in our thin film geometry. We confine the following discussion to room temperature, where k for typical glasses is well-described by k_{min}. We therefore need not consider the contribution from the "typical" non-diffusive phonon modes.

Wybourne and co-workers have presented a calculation for mean free path in boundary-limited phonon transport appropriate for samples of rectangular cross-section with high aspect ratio, $n = w/t$, where w is the width and t is the thickness of the Si-N bridge.[50,51] This is a modification of the usual Casimir limit of phonon boundary scattering appropriate for a bulk sample with square cross-sectional area. For all structures discussed in this paper $n = 70$. This allows calculation of the effective mean free path, $\ell_{\rm eff}$, when the top and bottom surfaces of the sample have different probabilities of diffuse reflection, f_1 and f_2 ($f = 1$ indicating entirely diffuse scattering and $f = 0$ entirely specular scattering). Reflections from the two much smaller area sides of the sample are assumed to always be diffuse. Note that the equations below include corrections specified by Wybourne, et al. in later work as well as our own corrections to ensure the definition of the aspect ratio is treated consistently. In this model $\ell_{\rm eff}$ is the sum of three terms:

$$\ell_{\rm eff} = \ell_0 + \frac{3t}{4n}\left\{\Sigma_{\rm odd} + \Sigma_{\rm even}\right\}, \tag{4}$$

where

$$\ell_0 = \frac{3t}{4n}\Big[\left(f_1 + f_2\right) I(n) + 2n^3 I\left(n^{-1}\right)\Big], \tag{5}$$

and the sums over either the odd indices $J = 1, 3, 5, ...$ and even indices $J = 2, 4, 6, ...$ are

$$\Sigma_{\rm odd} = \sum_{J=1,3,5,\ldots} \left(1-f_1\right)^{(J-1)/2}\left(1-f_2\right)^{(J-1)/2} \times$$
$$\Big\{\left[f_1\left(1-f_2\right) + f_2\left(1-f_1\right)\right]\alpha_J(n) + n^3\left[\left(1-f_1\right) + \left(1-f_2\right)\right]\beta_J\left(n\right)\Big\}, \tag{6}$$

and

$$\Sigma_{\rm even} = \sum_{J=2,4,6,\ldots} \left(1-f_1\right)^{J/2}\left(1-f_2\right)^{J/2}\Big[\left(f_1+f_2\right)\alpha_J(n) + 2n^3\beta_J\left(n\right)\Big], \tag{7}$$

where

$$I(r) = \frac{r}{2}\sinh^{-1}(r) + \frac{1}{6}\left[\left(1+r^2\right)^{1/2}\left(r^2-2\right) + \left(2-r^3\right)\right], \tag{8}$$

$$\alpha_J(n) = \left[(J+1)^3 I\left(\frac{n}{J+1}\right) - J^3 I\left(\frac{n}{J}\right)\right], \tag{9}$$

$$\beta_J(n) = \left[I\left(\frac{J+1}{n}\right) - 2I\left(\frac{J}{n}\right) + I\left(\frac{J-1}{n}\right)\right]. \tag{10}$$

Wybourne and others[52] have used this model to describe thermal transport at low temperatures where phonons are expected to scatter only at sample surfaces. Here we use it to describe the population of surface sensitive phonons in Si-N. The assumption that the large excess K above $K_{\rm min}$ at room temperature is due to the long ℓ modes can be written:

$$K_{\rm meas} - K_{\rm min} = \frac{1}{3}C_{\rm c}v_{\rm c}\ell_{\rm eff}, \tag{11}$$

where $K_{\rm meas}$ is the measured thermal conductance before addition of surface scattering centers, and $C_{\rm c}$ and $v_{\rm c}$ are the unknown heat capacity and sound velocity of the Casimir-like modes. The reasonable assumption that at a fixed temperature, both $C_{\rm c}$ and $v_{\rm c}$ are properties of the material itself and therefore independent of the surface treatment yields

$$\ell_{\rm eff}\left(f_1 = f_2, f_2\right) = \frac{K_{\rm meas} - K_{\rm min}}{K_{\rm sat} - K_{\rm min}}\ell_{\rm eff}\left(f_1 = 1, f_2\right), \tag{12}$$

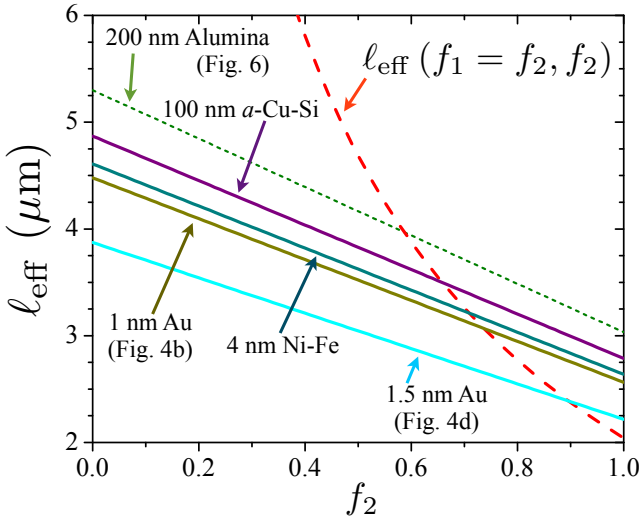

FIG. 8. $\ell_{\rm eff}$ vs f_2 allows graphic solution of Eq. 12 for 5 bridges. Note that the $\ell_{\rm eff}$ calculated from Eq. 4 even in the fully diffuse case for our geometry is ~ 2 μm.

Here $K_{\rm sat}$ is the room temperature K when all scattering at the top surface (where the film is added) is diffuse, and where we have explicitly included the dependence of $\ell_{\rm eff}$ on f_1 and f_2 for the two conditions of unaltered surfaces (where we assume $f_1 = f_2$) and surface scattering saturated at the top surface ($f_1 = 1$ and f_2 unaltered). As shown most clearly in Fig. 4d, $K_{\rm sat}$ is reached after the addition of ~ 1 nm of discontinuous Au.

As shown in Fig. 8, our measurements of $K_{\rm meas}$ and $K_{\rm sat}$ allow graphic solution of this transcendental equation for the unknown value f_2 and calculation of $\ell_{\rm eff}$. The two $\ell_{\rm eff}$ values are calculated as a function of f_2. We took 200 terms in the infinite sums in Eq. 4, which is more than adequate for values of f even as small as 0.01. The dashed line indicates $\ell_{\rm eff}$ calculated for $f_1 = f_2$, which depends only on the geometry of the bridge and f_2. The solid lines are the values of the right-hand side of Eq. 12 for various saturated bridge surfaces. Where a figure is indicated under the saturating film, results are described above. Note that $K_{\rm sat}$ for the alumina experiment was calculated assuming the initial alumina layer had the same actual k as the final alumina layer. K and k data for the other two cases are described elsewhere (a-Cu-Si[53], Ni-Fe[54]).

The intersections of the calculated $\ell_{\rm eff}\,(f_1 = f_2, f_2)$ with the other lines give the estimated value of f_2 and $\ell_{\rm eff}$ for each bridge. Three of these bridges have very similar values, with an average $f_2 = 0.7$ and average $\ell_{\rm eff} = 3.3$ μm. Note that the 1.5 nm saturating film experiment (shown in Fig. 4d) that shows somewhat higher $f_2 = 0.9$ and shorter $\ell_{\rm eff} = 2.7$ μm used a bridge fabricated from Si-N grown at UC Berkeley, indicating a possible, though slight, difference in the surface roughness of material from different CVD furnaces.

To estimate λ for this unusual population of phonons with $\ell = 3$ μm at room temperature requires additional information about the scattering centers added by the films to the Si-N surfaces. For the case of the discontinuous Au films, the average length scale of the surface roughness added to the Si-N by the Au islands can be determined from AFM images. Fig. 9 a) and b) compare AFM micrographs of the surface of a bare, as-grown Si-N film to the surface after growth of the 1 nm average thickness, discontinuous film with K shown in Fig. 4b. Both the scan area and the false color height scale is the same for both images, which were digitally leveled. Fig. 9c) shows the 1d roughness power spectral density determined from line-by-line Fourier transforms of the images as a function of inverse length, q (the top axis gives the associated real space length $2\pi/q$ in nm). The discontinuous Au film adds additional roughness for lengths of 20 nm and above. The RMS height roughness, η, for the two films determined from these scans is $\eta_{\rm Si-N} = 0.29$ nm for the bare Si-N and $\eta_{\rm Au} = 0.43$ nm for the Au-decorated surface.

Ziman's model of surface scattering[55] provides a means to estimate the wavelength of scattered phonons λ from f and η, the size of surface asperities:

$$(1 - f) = \exp\left(\frac{-16\pi^3\eta^2}{\lambda^2}\right). \tag{13}$$

Before addition of a film, f is determined by the surface roughness of the Si-N itself. With the values of $f = 0.7$ and $\eta_{\rm Si-N} = 0.29$ nm, this suggests an estimated phonon wavelength for the long ℓ excitations of $\lambda \sim 6$ nm. The approach in f to 1 caused by addition of the Au asperities suggests scattering of a somewhat shorter λ population

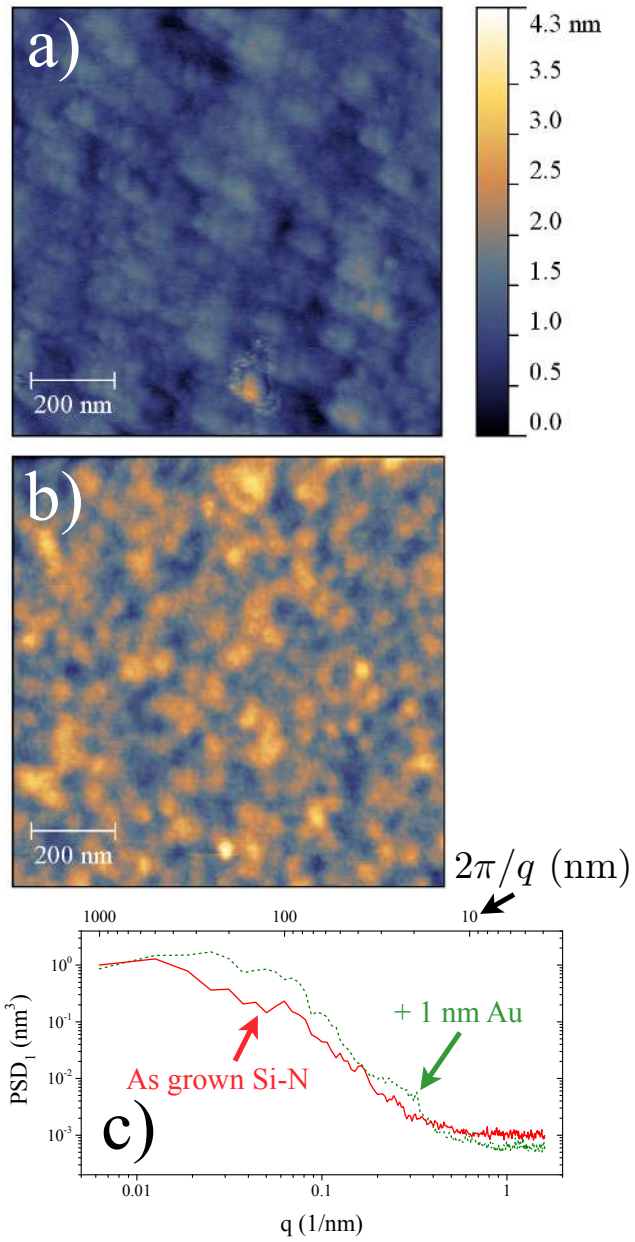

FIG. 9. AFM micrographs for **a)** bare 500 nm thick Si-N and **b)** Si-N coated with a discontinuous Au film with average thickness 1 nm. **c)** compares 1d roughness power spectral densities determined from the two images.

of phonons, with $\lambda \sim 4.5$ nm. Both scenarios involve phonons with λ much longer than the expected $\lambda_{\rm dom} \sim 0.2$ nm room temperature thermal phonons.

Finally, we estimate the fraction of the heat carried and the total heat capacity given by these long λ, long ℓ, efficient heat-carrying modes. One might be tempted to compare the reduction in total K caused by the additional surface scattering due to surface modification, $\Delta K = K_{\rm meas} - K_{\rm sat}$ to the original $K_{\rm meas}$. For the 4 bridges with $f_2 \approx 0.7$, ΔK is between 7 and 10 nw/K, which is $10-20$ % of the total K. This provides a conservative lower limit, but this simple method ignores the fact that the Casimir-like phonons carry heat effectively compared to other active modes at room temperature even when the surface scattering is totally diffuse. This argues that $K_{\rm meas} - K_{\rm min}$ is a better estimate of the heat carried by long λ, long ℓ modes at room temperature. As seen in Fig. 2, these values range from $20-30$ nW/K, representing $\sim 40-50\%$ of the total K. The total number of these modes can be estimated from the heat capacity $C_{\rm c}$. If the Casimir-like phonons have sound velocity $v_{\rm c}$ on the same order as the measured average $v_{\rm D}$, then $C_{\rm c}$ is given by Eq. 11. With $v_{\rm c} = v_{\rm D}$, $c_{\rm c} = 40$ μJ/g K. This is a tiny fraction of the 0.4 J/ g K total measured

room temperature specific heat of Si-N.[33] This shows that there are very few Casimir-like phonons, but that the very long ℓ allows them to carry large amounts of heat even at room temperature.

We can also use c_c as a second means to estimate λ of the Casimir-like phonon modes. A simple Debye specific heat calculation integrating only over modes with wavelength of λ_c or lower, again assuming sound velocity v_D and a Debye temperature of 985 K, gives ~ 40 μJ/g K for $\lambda_c = 10$ nm. This agrees well with the estimation of $\lambda \sim 6$ nm from the Ziman model (Eq. 13).

IV. CONCLUSION

We have presented results of several experiments that highlight the effect of long ℓ, long λ phonon surface scattering on thermal transport in micromachined Si-N bridges. Our results indicate that even in this relatively high temperature regime, introduction of diffuse phonon scattering causes a decrease in thermal conductance of Si-N bridges which causes an apparent decrease in the thermal conductivity of the Si-N. These experiments provide strong evidence that long ℓ vibrational modes contribute up to half the total heat conduction in disordered Si-N even at room temperature.

The effects of surface scattering of these long wavelength phonons on thermal transport in Si-N somewhat complicates the use of Si-N thermal platforms for measurements of the thermal conductivity of thin films (especially for low thermal conductivity thin films). However, the method we described here of measuring a series of film depositions on the same bridge reduces the error introduced by surface effects and allows reliable measurements of k. This was demonstrated through experiments on alumina and Au films that agreed well with either previously published values or the expectation of the Wiedemann-Franz law.

V. ACKNOWLEDGEMENTS

The authors would like to thank D. Queen and F. Hellman for providing Si-N grown at UC Berkeley, J. Beall, G. Hilton, and the Quantum Sensors Project at NIST Boulder for fabrication advice, assistance, and other useful discussions, and C. Leighton for advice on AFM roughness analysis. We also gratefully acknowledge support from the NSF (DMR-0847796, IIS-0813777), and DOE NA-22 (DE-FG52-09NA29359).

* barry.zink@du.edu

[1] T. Klitsner and R. O. Pohl, Physical Review B **36**, 6551 (1987).
[2] J. A. Johnson, A. A. Maznev, J. Cuffe, J. K. Eliason, A. J. Minnich, T. Kehoe, C. M. S. Torres, G. Chen, and K. A. Nelson, Phys. Rev. Lett. **110**, 025901 (2013).
[3] K. T. Regner, D. P. Sellan, Z. Su, C. H. Amon, A. J. H. McGaughey, and J. A. Malen, Nature Communications **4**, 1640 (2013).
[4] A. J. Minnich, Phys. Rev. Lett. **109**, 205901 (2012).
[5] A. J. Minnich, J. A. Johnson, A. J. Schmidt, K. Esfarjani, M. S. Dresselhaus, K. A. Nelson, and G. Chen, Phys. Rev. Lett. **107**, 095901 (2011).
[6] Y. K. Koh and D. G. Cahill, Phys. Rev. B **76**, 075207 (2007).
[7] X. Liu, J. L. Feldman, D. G. Cahill, R. S. Crandall, N. Bernstein, D. M. Photiadis, M. J. Mehl, and D. A. Papaconstantopoulos, Phys. Rev. Lett. **102**, 035901 (2009).
[8] Y. He, D. Donadio, and G. Galli, Applied Physics Letters **98**, 144101 (2011).
[9] A. I. Boukai, Y. Bunimovich, J. Tahir-Kheli, J.-K. Yu, W. A. Goddard, and J. R. Heath, Nature **451**, 168 (2008).
[10] A. I. Hochbaum, R. Chen, R. D. Delgado, W. Liang, E. C. Garnett, M. Najarian, A. Majumdar, and P. Yang, Nature **451**, 163 (2008).
[11] D. G. Cahill, W. K. Ford, K. E. Goodson, G. D. Mahan, A. Majumdar, H. J. Maris, R. Merlin, and S. R. Phillpot, Journal of Applied Physics **93**, 793 (2003).
[12] W. Holmes, J. M. Gildemeister, P. L. Richards, and V. Kotsubo, Applied Physics Letters **72**, 2250 (1998).
[13] R. Berman, E. L. Foster, and J. M. Ziman, Proceedings of the Royal Society of London Series A-Mathematical and Physical Sciences **231**, 130 (1955).
[14] Y. Shalibo, Y. Rofe, D. Shwa, F. Zeides, M. Neeley, J. M. Martinis, and N. Katz, Phys. Rev. Lett. **105**, 177001 (2010).
[15] S. Oh, K. Cicak, J. S. Kline, M. A. Sillanpää, K. D. Osborn, J. D. Whittaker, R. W. Simmonds, and D. P. Pappas, Phys. Rev. B **74**, 100502 (2006).
[16] L.-C. Ku and C. C. Yu, Physical Review B **72**, 024526 (2005).
[17] V. Keppens, B. C. Sales, D. Mandrus, B. C. Chakoumakos, and C. Laermans, Philosophical Magazine Letters **80**, 807 (2000).
[18] D. S. Swetz, P. A. R. Ade, M. Amiri, J. W. Appel, E. S. Battistelli, B. Burger, J. Chervenak, M. J. Devlin, S. R. Dicker, W. B. Doriese, R. Dnner, T. Essinger-Hileman, R. P. Fisher, J. W. Fowler, M. Halpern, M. Hasselfield, G. C. Hilton, A. D. Hincks, K. D. Irwin, N. Jarosik, M. Kaul, J. Klein, J. M. Lau, M. Limon, T. A. Marriage, D. Marsden, K. Martocci, P. Mauskopf, H. Moseley, C. B. Netterfield, M. D. Niemack, M. R. Nolta, L. A. Page, L. Parker, S. T. Staggs, O. Stryzak, E. R. Switzer, R. Thornton, C. Tucker, E. Wollack, and Y. Zhao, The Astrophysical Journal Supplement Series **194**, 41 (2011).
[19] S. Withington, D. J. Goldie, and A. V. Velichko, Phys. Rev. B **83**, 195418 (2011).
[20] C. Enss, ed., *Cryogenic Particle Detection*, Topics in Applied Physics, Vol. 99 (Springer-Verlag, Berlin Heidelberg, 2005).
[21] D. A. Bennett, R. D. Horansky, A. S. Hoover, N. J. Hoteling, M. W. Rabin, D. R. Schmidt, D. S. Swetz, L. R. Vale, and J. N. Ullom, Applied Physics Letters **97**, 102504 (2010).
[22] R. D. Horansky, J. N. Ullom, J. A. Beall, G. C. Hilton, K. D. Irwin, D. E. Dry, E. P. Hastings, S. P. Lamont, C. R. Rudy, and M. W. Rabin, Applied Physics Letters **93**, 123504 (2008).
[23] K. D. Irwin and G. C. Hilton, "Transition-edge sensors," in *Cryogenic Particle Detection*, Topics in Applied Physics, Vol. 99, edited by C. Enss (Springer-Verlag, Berlin Heidelberg, 2005) pp. 63–149.
[24] P. J. French, P. M. Sarro, R. Mallée, E. J. M. Fakkeldij, and R. F. Wolffenbuttel, Sensors and Actuators A **58**, 149 (1997).
[25] C. H. Mastrangelo, Y.-C. Tai, and R. S. Muller, Sensors and Actuators A **A23**, 856 (1990).
[26] D. W. Denlinger, E. N. Abarra, K. Allen, P. W. Rooney, M. T. Messer, S. K. Watson, and F. Hellman, Review of Scientific Instruments **65**, 946 (1994).
[27] E. A. Olson, M. Y. Efremov, A. T. Kwan, S. Lai, V. Petrova, F. Schiettekatte, J. T. Warren, M. Zhang, and L. H. Allen, Applied Physics Letters **77**, 2671 (2000).
[28] M. Zhang, M. Y. Efremov, E. A. Olson, Z. S. Zhang, and L. H. Allen, Applied Physics Letters **81**, 3801 (2002).
[29] B. Revaz, B. L. Zink, and F. Hellman, Thermochimica Acta **432**, 158 (2005).
[30] R. Sultan, A. D. Avery, G. Stiehl, and B. L. Zink, Journal of Applied Physics **105**, 043501 (2009).
[31] B. L. Zink, A. D. Avery, R. Sultan, D. Bassett, and M. R. Pufall, Solid State Communications **150**, 514 (2010).
[32] A. D. Avery, R. Sultan, D. Bassett, D. Wei, and B. L. Zink, Physical Review B **83**, 100401 (2011).
[33] B. L. Zink and F. Hellman, Solid State Communications **129**, 199 (2004).
[34] Available at gwyddion.net.
[35] S. T. Huxtable, (private communication).
[36] D. R. Queen and F. Hellman, Review of Scientific Instruments **80**, 063901 (2009).
[37] A. Sikora, H. Ftouni, J. Richard, C. Hebert, D. Eon, F. Omnes, and O. Bourgeois, Review of Scientific Instruments **83**, 054902 (2012).
[38] S. M. Lee and D. G. Cahill, Journal of Applied Physics **81**, 2590 (1997).
[39] S. K. Watson and R. O. Pohl, Physical Review B **68**, 104203 (2003).
[40] R. C. Zeller and R. O. Pohl, Physical Review B **4**, 2029 (1971).

[41] D. G. Cahill, S. K. Watson, and R. O. Pohl, Phys. Rev. B **46**, 6131 (1992).
[42] D. G. Cahill and R. Pohl, Solid State Communications **70**, 927 (1989).
[43] S. Wenzel, Ph.D. thesis, University of California, Berkeley (1992).
[44] F. J. Bermejo, E. Enciso, A. Criado, J. L. Martínez, and M. Garcia-Hernández, Phys. Rev. B **49**, 8689 (1994).
[45] R. Wawryk, C. Marucha, K. Balcerek, B. M. Terzijska, and Z. G. Ivanova, Cryogenics **40**, 749 (2000).
[46] B. Ganapathysubramanian and N. Zabaras, Computer Methods in Applied Mechanics and Engineering **197**, 3560 (2008).
[47] B. L. Zink, B. Revaz, J. J. Cherry, and F. Hellman, Review of Scientific Instruments **76**, 024901 (2005).
[48] I. Stark, M. Stordeur, and F. Syrowatka, Thin Solid Films **226**, 185 (1993).
[49] D. G. Cahill, Bulletin of the Materials Research Society **37**, 855 (2012).
[50] M. N. Wybourne, C. G. Eddison, and M. J. Kelly, Journal of Physics C: Solid State Physics **17**, L607 (1984).
[51] C. G. Eddison and M. N. Wybourne, Journal of Physics C: Solid State Physics **18**, 5225 (1985).
[52] G. Wang, V. Yefremenko, V. Novosad, A. Datesman, J. Pearson, R. Divan, C. L. Chang, L. Bleem, A. T. Crites, J. Mehl, T. Natoli, J. McMahon, J. Sayre, J. Ruhl, S. S. Meyer, and J. E. Carlstrom, IEEE Transactions on Applied Superconductivity **21**, 232 (2011).
[53] R. Sultan, Ph.D. thesis, University of Denver (2010).
[54] A. D. Avery, Ph.D. thesis, University of Denver (2013).
[55] J. M. Ziman, *Electrons and phonons : the theory of transport phenomena in solids.* (Clarendon Press., Oxford, 1960).